

0.0.1 Fundamentals and Applications of Isotope Effect in Modern Technology.

V.G. Plekhanov.

Fonoriton Science Lab., Garon Ltd., P.O. Box 2632, Tallinn, 13802, ESTONIA

<e-mail> vgplekhanov@hotmail.com

Different crystals (semiconductors and insulators) with varying isotopic composition have been recently grown. I discuss here the effect of isotopic mass and isotopic disorder on the properties (vibrational, elastic, thermal and optical) of different crystals. The main applications of the stable isotopes are included self-diffusion, neutron transmutative doping (NTD) of different semiconductors, optical fibers, isotope-based quantum computers, etc. Because of space limitations this discussion will not be exhaustive. I hope however, to give sufficient references to published work so that the interested reader can easily find the primary literature sources to this rapidly expanding field of solid state physics.

Phonons, excitons, isotope-mixed crystals, laser materials, quantum information, isotope-based quantum computers.

It is well-known that the presence of randomly distributed impurities in a crystal can give rise to significant variations of its mechanical, electrical, thermal, and optical properties with respect to those of the pure solid. All these properties are, more or less, directly related to the structure of the manifold of phonon states and any variation induced in this structure by the presence of the impurities, will produce a corresponding alteration of the physical properties of the material. Of particular interest is the case in which the impurity species is of the same chemical nature, but with a different mass, i.e. the case of isotopic impurities. The mechanisms by which the impurities (isotopes) perturb the phonon distribution will depend on the mass difference between the host and guest species [1-3]. Phonons are the crystal excitations most directly related to the isotopic

masses. In monatomic crystals (like C, Ge, Si., etc.), and within the harmonic approximation, all phonon frequencies scale like the square root of the average isotopic mass. Namely, this feature can be used for the nondestructive isotopic characterization investigated materials. The isotopic effect can be classified into two categories: 1) The first type is caused by the variation of the phonon frequencies with the average isotopic mass. To this type belongs the isotope effect in superconductors, which plays an important role in the search for the mechanism of high T_c superconductivity (see, e.g. [4]). The effect of changing the atomic mass M is to change the phonon frequencies ω according to:

$$\omega = \sqrt{\frac{\alpha}{M}}, \quad (1)$$

where α is a force constant characteristic of the phonon under consideration. The change in atomic mass implies, at low temperatures (see below), a change in the average atomic displacement for each phonon mode. In the case of one atom per primitive cell the mean squared phonon amplitude $\langle u^2 \rangle$ is given by [1;2]:

$$\langle u^2 \rangle = \frac{\langle \frac{\hbar^2}{4M\omega} [1 + 2n_B(\omega)] \rangle}{\langle \frac{\hbar}{4M^{1/2}\alpha^{1/2}} [1 + 2n_B(\omega)] \rangle}, \quad (2)$$

where $n_B(\omega)$ is the Bose - Einstein statistical factor, ω is the frequency of a given phonon and $\langle \dots \rangle$ represents an average over all phonon modes. The average in r.h.s. of (2) is often simplified by taking the value inside $\langle \dots \rangle$ at an average frequency ω_D which usually turns out to be close to the Debye frequency. We should distinguish between the low temperature ($\hbar\omega \gg k_B T$) and the high temperature ($\hbar\omega \ll k_B T$) limits and see:

$$\begin{aligned} (\hbar\omega \gg k_B T), \quad \langle u^2 \rangle &= \frac{\hbar}{4M\omega_D} \sim M^{-1/2} \\ \text{independent of } T \text{ and} \\ (\hbar\omega \ll k_B T), \quad \langle u^2 \rangle &= \frac{k_B T}{2M\omega^2} \sim T \\ \text{independent of } M \end{aligned} \quad (3).$$

Using Eq. (1) we can find from last equations that $\langle u^2 \rangle$, the zero-point vibrational amplitude, is proportional to $M^{-1/2}$ at low temperatures: it thus decreases with increasing M and vanishes for $M \rightarrow \infty$. For high T , however, we find that $\langle u^2 \rangle$ is independent of M and linear in T (details see [3] and references therein).

Another type of isotope effects is produced by the

isotopic mass fluctuations about the average mass $\langle M \rangle$. These fluctuations perturb the translational invariance of a crystal and lift, at least in part, \mathbf{k} - vector conservation. The most striking effect of this type is observed in the thermal conductivity which has a maximum at a temperature $T_M \ll \Theta_D$ (here Θ_D is Debye temperature, $T_M = 80$ K for diamond, $T_M = 20$ K for silicon (see, also Figs. 64 - 66 in [3]). Reduction of the concentration of ^{13}C from the standard 1% (against 99% of ^{12}C) by a factor of ten increases the thermal conductivity of diamond by about a factor of two, a fact that leads to amplifications in situations where a large amount of generated heat has to be driven away (e.g. as substrates for high power electronic devices [5]). As is well-known this maximum represents the transition from boundary scattering to the phonon unklapp scattering regime and its value K_m is determined by the isotopic fluctuation parameter g (mass variance):

$$g = \frac{\langle M^2 \rangle}{\langle M \rangle^2} - 1,$$

the larger g - the smaller K_m [6].

It is known that materials having a diamond structure are characterized by the triply degenerate phonon states in the Γ - point of the Brillouin zone ($\mathbf{k} = 0$). These phonons are active in the Raman scattering (RS) spectra, but not in the IR absorption ones (see, e.g. [7]). First - order Raman light - scattering spectrum in diamond crystals includes one line with the maximum at $\omega_{LTO}(\Gamma) = 1332.5 \text{ cm}^{-1}$. In Fig. 1^a, the first-order scattering spectrum in diamond crystals with different isotope concentration is shown [8]. As was shown, the maximum and the width of the first-order scattering line in isotopically-mixed diamond crystals are nonlinearly dependent on the concentration of isotopes x (see also [7]). The maximum shift of this line is 52.3 cm^{-1} , corresponding to the limiting values of $x = 0$ and $x = 1$.

Fig. 1^b demonstrates the dependence of the shape and position of the first-order line of optical phonons in germanium crystal on the isotope composition at liquid nitrogen temperatures [9]. The coordinate of the center of the scattering line is proportional to the square root of the reduced mass of the unit cell, i.e. $M^{-1/2}$. It is precisely this dependence that is expected in the harmonic approximation (details

see [3]). An additional frequency shift of the line is observed for the natural and enriched germanium specimens and is equal, as shown in Refs. [7, 9] to 0.34 ± 0.04 and $1.06 \pm 0.04 \text{ cm}^{-1}$, respectively (see also Fig. 7 in Chap. 4 of Ref. [10]). Detailed calculation of the shape of the lines in RS of semiconductors have been performed by Spitzer et al. [11]. In their paper a quantitative agreement with the experimental data on diamond and germanium has been obtained. Comparing the half-widths of the scattering lines in first-order RS in diamond and germanium (see Fig. 1), it is easy to see that the observed line broadening due to isotopic disorder in diamond is much greater than that in germanium. The reason for this is that the $\mathbf{k} = 0$ point is not the highest point in the diamond dispersion curve (see Fig. 10^b in Ref. [7]), whereas in the case of germanium it is the highest point [12]. This shift of the maximum from the Γ - point ($\mathbf{k} = 0$) leads to a much larger density of states in the vicinity of ω_{LTO} in comparison with the normal one calculated by the formula:

$$N_d \sim \text{Re}(\omega_{LTO} - \omega + i[\frac{\Delta\omega_{LTO}}{2}])^{1/2} \quad (4)$$

(for more details see Ref. [12]). The density of states in diamond is asymmetric with respect to ω_{LTO} , causing asymmetry in the shape of the scattering line [7]. This asymmetry also leads to the asymmetric concentration dependence of the half-width of the scattering line. As was shown early (see, e.g. [3] and references therein), in the case of a weak potential of isotopic scattering of phonons, their self-energy $\varepsilon(\omega)$ does not depend on \mathbf{q} (- phonon quasiimpuls). This is precisely the situation observed for C and Ge. Indeed, if we express the mass fluctuation $\Delta M/\bar{M}$ (\bar{M} is the mean mass of all isotopes) in the form of the variation of the phonon band width $\Delta\omega_0 = 12 \text{ cm}^{-1}$ at $\mathbf{q} = 0$ and compare it with the width of the band of optical phonons in Ge equals to $\approx 100 \text{ cm}^{-1}$, we will see that the variations very small. Under this conditions the localization of optical phonons in Ge is naturally, absent, and as observed in experiment, they stay delocalized (see below, however opposite case in $\text{LiH}_x\text{D}_{1-x}$ crystals). Moreover, direct measurements of the phonon lifetime in Ge show that, in the case of anharmonic decay, it is two orders of magnitude shorter than the lifetime that is due to the ad-

ditional scattering by isotopes, i.e. $\tau_{anhar} = \tau_{disord} \cdot 10^{-2}$ [13]. Therefore, the contribution of anharmonicity to the half-width of the first-order light scattering line in Ge is two orders of magnitude greater than that caused by the isotopic disorder in crystal lattice. In conclusion of this part of our report we should mention that analogous structure of first-order RS and their dependence on isotope composition has by now been observed many times, not only in elementary Si and α -Sn, but also in compound CuCl, CuBr, ZnSe, GaN semiconductors (details see Ref. [3]).

In Fig. 2 (curve 1) the spectrum of second-order RS of light in pure LiD crystal is shown [7]. In spite of the fact, according to the nomogram of exciton states [14], the crystal studied should be considered to be pure, its RS spectrum contains a clear high-frequency peak around 1850 cm^{-1} . The observed peak does not have an analogue in RS of pure LiH (Fig. 2, curve 4) and has already been observed earlier in the second-order RS and has been interpreted (see [7] and references therein) as a local vibration of the hydrogen in LiD crystals. Further we note that as the concentration grows further ($x > 0.15$) one observes in the spectra a decreasing intensity in the maximum of $2\text{LO}(\Gamma)$ phonons in LiD crystal with a simultaneous growth in intensity of the highest frequency peak in mixed $\text{LiH}_x\text{D}_{1-x}$ crystals (Fig. 2, curve 3). The origin of the last one is in the renormalization of $\text{LO}(\Gamma)$ vibrations in mixed crystals [7]. Comparison of the structure of RS spectra (curves 1 and 2 in Fig. 2) allows us, therefore, to conclude that in the concentration range of $0.1 < x < 0.45$ the RS spectra simultaneously contain peaks of the $\text{LO}(\Gamma)$ phonon of pure LiD and the $\text{LO}(\Gamma)$ phonon of the mixed $\text{LiH}_x\text{D}_{1-x}$ crystal. Thus, the second-order RS spectra of $\text{LiH}_x\text{D}_{1-x}$ crystals have one- and two-mode character for $\text{LO}(\Gamma)$ phonons, and also contain a contribution from the local excitation at small values of x . Moreover, we should add that an additional structure in RS spectra on the short-side of the $2\text{LO}(\Gamma)$ peak (see Fig. 21 in Ref. [7]) was observed relatively ago in mixed $\text{LiH}_x\text{D}_{1-x}$ crystals and, very recently, in isotopically mixed crystals of diamond, germanium and α -Sn (details see [3, 11]). These effects caused by isotopic disorder in the crystal lattice of isotopically mixed crystals [3]. The observation of two-

mode behavior of the $\text{LO}(\Gamma)$ phonons in RS spectra of $\text{LiH}_x\text{D}_{1-x}$ crystals contradicts the prediction of the CPA [15], according to which the width W of optical vibration band should be smaller than the frequency shift (Δ) of transverse optical phonon. However, as was shown early (see, e.g. [7] and references therein) in $\text{LiH}_x\text{D}_{1-x}$ mixed crystals, the reverse inequality is valid, i.e. $W > |\Delta|$. According [16], this discrepancy between experimental results and theory based on CPA [15] is mainly explained by the strong potential of scattering of phonons, caused by a large change in the mass upon substitution of deuterium for hydrogen. Once more reason of the discrepancy between theory and results of the experiment may be connected with not taking into account in theory the change of the force-constant at the isotope substitution of the smaller in size D by H ion. We should stress once more that among the various possible isotope substitution, by far the most important in vibrational spectroscopy is the substitution of hydrogen by deuterium. As is well-known, in the limit of the Born-Oppenheimer approximation the force-constant calculated at the minimum of the total energy depends upon the electronic structure and not upon the mass of the atoms. It is usually assumed that the theoretical values of the phonon frequencies depend upon the force-constants determined at the minimum of the adiabatic potential energy surface. This leads to a theoretical ratio $\omega(\text{H})/\omega(\text{D})$ of the phonon frequencies that always exceed the experimental data. Very often anharmonicity has been proposed to be responsible for lower value of this ratio. In isotope effect two different species of the same atom will have different vibrational frequencies only because of the difference in isotopic masses. The ratio p of the optical phonon frequencies for LiH and LiD crystals is given in harmonic approximation by:

$$p = \frac{\omega(\text{H})}{\omega(\text{D})} = \sqrt{\frac{M(\text{LiD})}{M(\text{LiH})}} \simeq \sqrt{2} \quad (6)$$

while the experimental value (which includes anharmonic effects) is $1.396 \div 1.288$ (see Table in Ref. [17]). In this Table there are the experimental and theoretical values of p according to formula (6), as well as the deviation $\delta = \frac{p_{\text{theory}} - p_{\text{exp}}}{p_{\text{theory}}}$ of these values from theoretical ones. Using the least squares method it was found the empirical formula of $\ln(\delta\%)$

$\sim f(\ln[\frac{\partial E}{\partial M}])$ which is depicted on Fig.3. As can be seen the indicated dependence has in the first approximation a linear character:

$$\ln(\delta\%) = -7.5 + 2\ln(\frac{\partial E}{\partial M}). \quad (7)$$

From the results of Fig. 3, it can be concluded that only hydrogen compounds (and its isotope analog - deuterium) need to take into account the force-constant changes in isotope effect. It is also seen that for semiconductor compounds (on Fig. 3 - points, which is below of Ox line) the isotope effect has only the changes of the isotope mass (details see [3, 7]).

The dependence of the band gap energy on isotopic composition (via mechanism of electron-phonon interaction) has already been observed for insulators (Fig. 4) and lowest (indirect - direct) gap of different semiconductors ([3] and references therein). It has been shown to result primarily from the effect of the average isotopic mass on the electron-phonon interaction, with a smaller contribution from the change in lattice constant. It was the first paper [19] where the exciton binding energy E_B was found to depend on the isotopic composition. It was shown further that this change in E_B was attributed to the exciton-phonon interaction (originally with LO phonons) (see, also [3]). At present time such dependence of $E_B \sim f(x)$ (x - isotope concentration) was found for different bound excitons in semiconductors [20 - 21]. The simplest approximation, in which crystals of mixed isotopic composition are treated as crystals of identical atoms having the average isotopic mass is referred to as virtual crystal approximation (VCA) [15]. Going beyond the VCA, in isotopically mixed crystals one would also expect local fluctuations in the band-gap energy from statistical fluctuations in local isotopic composition within some effective volume, such as that of an exciton (see, e.g. Fig. 2 of Ref. [18]). Using the least-squares method it was found the empirical dependence of $\ln(\frac{\partial E_g}{\partial M}) \sim f(\ln E_g)$, which is presented on Fig. 5. As can be seen the mentioned dependence has a parabolic character:

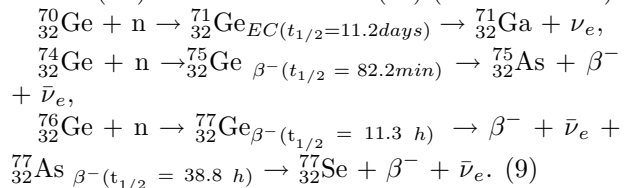
$$\ln(\frac{\partial E_g}{\partial M}) = 6.105(\ln E_g)^2 - 7.870(\ln E_g) + 0.565. \quad (8)$$

From this figure it can be concluded also that the small variation of the nuclear mass (semiconductors) causes the small changes in E_g also. When the nu-

clear mass increases it causes the large changes in E_g (C, LiH, CsH, etc.) (details, see [18, 3]).

Detail analyze the process of self-diffusion in isotope pure materials and hetero-structures was done in [5]. Interest in diffusion in solids is as old as metallurgy or ceramics, but the scientific study of the phenomenon may probably be dated some sixth-seven decades ago. As is well-known, the measured diffusion coefficients depends on the chemistry and structure of the sample on which it is measured. In cited paper [5] it was shown to use the stable isotopes for the study of diffusion process in different semiconducting structures (bulk, hetero-structures etc.).

Chapter 6 indicated book [5] describes the new reactor technology - neutron transmutative doping (NTD). Capture of thermal neutrons by isotope nuclei followed by nuclear decay produces new elements, resulting in a very number of possibilities for isotope selective doping of solids. The importance of NTD technology for studies of the semiconductor doping as well as metal-insulator transitions and neutral impurity scattering process is underlined. The low-temperature mobility of free carriers in semiconductors is mainly determined by ionized- and neutral-impurity scattering. The ionized-impurity scattering mechanism has been extensively studied (see e.g. [5] and references therein), and various aspects of this process are now quite well understood. Scattering by neutral impurities is much less than by ionized centers, i.e., its contribution is significant only in crystals with low compensation and at very low temperatures where most of the free carriers are frozen on the impurity sites. The availability of highly enriched isotopes of Ge which can be purified to residual dopant levels $< 10^{12} \text{ cm}^{-3}$ has provided the first opportunity to measure neutral impurity scattering over a wide temperature range. In paper [22] three Ge isotopes transmute into shallow acceptors (Ga), shallow donors (As) and double donors (Se) (see also above):



The isotopes ${}^{72}\text{Ge}$ and ${}^{73}\text{Ge}$ are transmuted into

the stable ^{73}Ge and ^{74}Ge respectively. Controlling the ratio of ^{70}Ge and ^{74}Ge in bulk Ge crystals allows fine tuning of the majority- as well as the minority carrier concentration. Currently, this is the best method to vary the free-carrier concentration independently from compensation ratio. As opposed to other doping methods, NTD yields a very homogeneous, perfectly random distribution of the dopants down to the atomic levels [5]. Thus isotopically controlled crystals offer a unique possibility to study systematically the scattering mechanism of the charge carriers in semiconductors. Extensive Hall-effect and resistivity measurements from room temperature down to 4.2K yielded very accurate free-carrier concentrations and mobilities as a function of temperature and doping level were done in paper [5]. Itoh et al. [22] have performed temperature-dependent Hall measurements on four different p-type and two-different n-type Ge crystals (Fig. 6). Fig. 6 shows the relative strength of the scattering from the ionized and the neutral impurities. There is only a relatively small temperature region in which the scattering from the neutral impurities dominates. This range extends to higher temperatures as the free-carrier concentration is increased. The calculated "transition temperatures" above which the ionized impurities are the main scattering centres compare very well with experimental results of Itoh et al [22] (see also Fig. 6.31 in Ref. [5]). In order to demonstrate the importance of the homogeneous dopant distribution, Itoh et al. have performed the same study on samples cut from Ge : Ga crystals grown by the conventional Czochralski method, where Ga impurities were introduced to Ge melt during the crystal growth. These authors observed deviations of the measured mobility from the theoretical calculations, which are most likely due to inhomogeneous Ga impurity distributions in melt-doped Ge. Only the use of NTD semiconductors with randomly distributed dopants allows for an accurate test of the neutral impurity-scattering models (details, see [5]).

Another application of isotope pure and isotope mixed crystals that will be discussed here is related to the possibility of using an isotopically mixed medium (e.g. $\text{LiH}_x\text{D}_{1-x}$ or $^{12}\text{C}_x\text{ }^{13}\text{C}_{1-x}$) as an oscillator of coherent radiation in the ultraviolet spectral range.

To achieve this, the use of indirect electron transitions involving, say, LO phonons was planned [23]. The detection of LO phonon replicas of free - exciton luminescence in wide - gap insulators attracted considerable attention to these crystals (see e.g. [10; 23]). At the same time it is allowed one to pose a question about the possibility of obtaining stimulated emission in UV (VUV) region (4 - 6 eV) of the spectrum, where no solid state sources for coherent radiation exist yet. In the first place this related to the emitters working on the transitions of the intrinsic electronic excitation (exciton). The last one provides the high energetical yield of the coherent emission per unit volume of the substance.

In this part we will discuss the investigation results of the influence of the excitation light density on the resonant secondary emission spectra of the free - exciton in the wide - gap insulator $\text{LiH}_x\text{D}_{1-x}$ ($\text{LiH}_{1-x}\text{F}_x$) crystals. The cubic LiH crystals are typical wide - gap ionic insulator with $E_g = 4.992$ eV [10] with relatively weak exciton - phonon interaction however: $E_B/\hbar\omega_{LO} = 0.29$ where E_B and $\hbar\omega_{LO}$ are exciton binding energy and longitudinal optical phonon's energy, respectively. Besides it might be pointed out that the analogous relation for CdS, diamond and NaI is 0.73; 0.45 and 12.7, respectively. In the insert of Fig. 7 depicts the luminescence of 1LO and 2LO phonon replicas in LiH crystals. An increase in the density of the exciting light causes a burst of the radiation energy in the long-wave wing of the emission of the 1LO and 2LO repetitions (see Fig. 7) at a rate is higher for the 1LO replica line [23]. A detailed dependence of the luminescence intensity and the shape of the 2LO phonon replica line are presented in Fig. 7. The further investigations have shown [5] that with the increase of the excitation light intensity at the beginning a certain narrowing can be observed, followed by widening of the line of 2LO phonon replica with a simultaneous appearance of a characteristics, probably mode structure (see Fig. 8.11 in Ref. [5]). From this Fig. it can be seen that the coupling between longwavelength luminescence intensity and excitation light intensity is not only linear, but, in fact, of a threshold character as in case of other crystals. A proximity of the exciton parameters of LiH and CdS (ZnO) crystals allowed to

carry out the interpretation of the density effects in LiH on the analogy with these semiconducting compounds. Coming from this in the paper [23] it was shown that for the observed experimental picture on LiH crystals to suppose the exciton-phonon mechanism of light generation [5] is enough the excitons density about 10^{15} cm^{-3} . This is reasonable value, if the high quality of the resonator mirror - the crystal cleavage "in situ" and relatively large exciton radius ($r = 40 \text{ \AA}$ [10]) is taken into account. To this light mechanism generation must be also promoting a large value of the LO phonon energy ($\hbar\omega_{LO} = 140 \text{ meV}$). Owing to this the radiative transition is being realized in the spectral region with a small value of the absorption coefficient, and thus with a small losses in resonator (details see [5]).

In conclusion of this section we should underlined that if the observable mode structure is really caused by the laser generation it may be smoothly tuned in the region of energies $4.5 \pm 5.1 \text{ eV}$ owing to smooth transition of the line emission energy in the $\text{LiH}_x\text{D}_{1-x}$ ($\text{LiH}_x\text{F}_{1-x}$; $\text{LiD}_x\text{F}_{1-x}$) mixed crystals as well as in the range $5.35 - 5.10 \text{ eV}$ in $^{12}\text{C}_x\text{ }^{13}\text{C}_{1-x}$ mixed crystals (see also [10]).

Concluding our report we should be paid your attention to the reports of Professors Schoven, Weston, Wendt as well as Dr. Chai of our conference which are devoted in the first step of radioactive isotope applications.

Figure Captions.

Fig. 1. a) First-order Raman spectra of $^{12}\text{C}_x^{13}\text{C}_{1-x}$ diamonds with different isotope compositions. The labels A,B, C, D, E and F correspond to $x = 0.989$; 0.90 ; 0.60 ; 0.50 ; 0.30 and 0.01 respectively. The intensity is normalized at each peak (after [8]); b) First-order Raman scattering spectra in Ge with different isotope contents (after [13]).

Fig. 2. Second-order Raman spectra of $\text{LiH}_x\text{D}_{1-x}$ crystals at room temperature: (1); (2); (3) and (4) $x = 0$; 0.42 ; 0.76 and 1 , respectively (after [7]).

Fig. 3. The dependence of $\ln(\delta\%) \sim f(\ln[\frac{\partial E_g}{\partial M}])$: points are experimental values and continuous line - calculation on the formula (7) (after [17]).

Fig. 4. Mirror reflection spectra of crystals: LiH, curve 1; $\text{LiH}_x\text{D}_{1-x}$, curve 2 and LiD, curve 3 at 4.2

K. Light source without crystals, curve 4 (after [18]).

Fig. 5. The dependence of $\ln(\frac{\partial E_g}{\partial M}) \sim f(\ln E_g)$: points are experimental data and continuous line - calculation on the formula (8) (after [18]).

Fig. 6. Temperature dependence of the carrier mobility of a) p - type and b) n - type NTD Ge crystals. c) Temperature dependence of relative contributions to the mobility. Note that the mobility is dominated by neutral impurity scattering below 20 K ($^{70}\text{Ge}:\text{Ga} \# 2$ crystal) (after [22]).

Fig. 7. The dependence of the intensity in the maximum (1) and on the long-wavelength side (2) of 2LO replica emission line of LiH crystals on the excitation light intensity. In insert: luminescence spectra of free excitons in LiH crystals in the region of the emission lines of 1LO and 2LO phonon repetitions at 4.2 K for low (1) and high (2) density of excitations of 4.99 eV photons (after [23]).

References.

1. I.M. Lifshitz, *Physics of Real Crystals and Disordered Systems*, Selected Works (Eds. M.I. Kaganov, A.M. Kosevich, Science, Moscow, 1987) (in Russian).
2. A.A. Maradudin, E.W. Montroll, G.H. Weiss and I.P. Ipatova, *Theory of Lattice Dynamics in the Harmonic Approximation*, Solid State Physics, Vol.3, (Eds. F. Seitz, D. Turnbull and H. Ehrenreich, Academic, New York, 1971).
3. V.G. Plekhanov, Elementary Excitations in Isotope-Mixed Crystals, *Physics Reports*, **410** [1-3] 1 (2005).
4. J.P. Franck, in: *Physical Properties of High T_c Superconductors* (ed. D.M. Ginsberg, Vol. 4., World Scientific, Singapore, 1984) p. 189.
5. For a review, see, V.G. Plekhanov, *Applications of the Isotopic Effect in Solids*, Springer, Berlin - Heidelberg, 2004.
6. See, for example, R. Berman, *Thermal Conduction of Solids* (Clarendon Press, Oxford, 1976); T.M. Tritt, *Thermal Conductivity* (Springer, Berlin - Heidelberg, 2005).
7. V.G. Plekhanov, Isotopic Effects in Lattice Dynamics, *Physics - Uspekhi* (Moscow) **46** [7] 689 (2003).

8. H. Hanzawa, N. Umemura, Y. Nisida et al., Disorder Effects of Nitrogen Impurities, Irradiation - Induced Defects, and ^{13}C Isotope Composition on the Raman Spectrum in Synthetic I^b Diamond, *Phys. Rev.* **B54** [6] 3793 (1996).

9. M. Cardona, Semiconductor Crystals with Tailor - Made Isotopic Compositions, in: *Festkorperprobleme/Advances in Solid State Physics* (ed. R. Helbig, Vieweg, Braunschweig, Wiesbaden, Vol. 34, 1994) p. 35.

10. V.G. Plekhanov, *Isotope Effects in Solid State Physics* (Academic, New York, 2001).

11. J. Spitzer, P. Etchegoin, M. Cardona et al., Isotopic - Disorder Induced Raman Scattering in Diamond, *Solid State Commun.* **88** [6] 509 (1993).

12. M. Cardona, Isotopic Effects in the Phonon and Electron Dispersion Relations of Crystals, *Phys. Stat. Sol. (b)* **220** [1] 5 (2000).

13. M. Cardona, P. Etchegoin, H.D. Fuchs et al., Effect of Isotopic Disorder and Mass on the Electronic and Vibronic Properties of Three-, Two- and One - Dimensional Solids, *J. Phys.: Condens. Matter* **5** [1] A61 (1993).

14. V.G. Plekhanov, Phonon renormalization of Interband Transition Energy in the Mixed Crystals, *Solid State Commun.* **76** [1] 51 (1990).

15. R.J. Elliott, J.A. Krumhansl and P.L. Leath, The Theory and Properties of Randomly Disordered Crystals and Related Physical Systems, *Rev. Mod. Phys.* **46** [3] 465 (1974).

16. V.G. Plekhanov, Experimental Evidence of Strong Phonon Scattering in Isotope Disordered Systems: The Case of $\text{LiH}_x\text{D}_{1-x}$, *Phys. Rev.* **B51** [14] 8874 (1995).

17. V.G. Plekhanov (unpublished results, 2004)

18. V.G. Plekhanov, N.V. Plekhanov, Isotope Dependence of Band - Gap Energy, *Phys. Lett.*, **A313** [3] 231 (2003).

19. V.G. Plekhanov, T.A. Betenekova, V.A. Pustovarov, Excitons and Peculiarities of Exciton-Phonon Interaction in LiH and LiD, *Sov. Phys. Solid State* **18** [8] 1422 (1976).

20. M. Cardona, Dependence of the Excitation Energies of Boron in Diamond on Isotopic Mass, *Solid State Commun.* **121** [1] 7 (2002).

21. D. Karaickaj, T.A. Meyer, M.L.W. Thewalt et al., Dependence of the Ionization Energy of Shallow Donors and Acceptors in Silicon on the Host Isotopic Mass, *Phys. Rev.* **B68** [2] 121201 (2003).

22. H.D. Fuchs, K.M. Itoh and E.E. Haller, Isotopically Controlled Germanium: A New Medium for the Study of Carrier Scattering by Neutral Impurities, *Philos. Mag.* **B70** [2] 662 (1994); K.M. Itoh, E.E. Haller, V.I. Ozogin, Neutral - Impurity Scattering in Isotopically Engineered Ge, *Phys. Rev.* **B50** [23] 16995 (1994).

23. V.G. Plekhanov, Wide-Gap Insulators Excitonic Nonlinearity and Its Potential Applications in Solid State Lasers, in: *Proc. Int. Conf. Advances Solid State Lasers*, USA, SOQUE, 1990.

Table. Values of the coefficients dE/dM (meV, cm^{-1}) for the optical phonons and the experimental and theoretical values of p as well as deviation $\delta\%$ of these values from theoretical ones.

Substances	Frequencies	p_{exp}
LiH/LiD	140(meV)/104(meV)[10,24]	1.288-1.346
$\text{SiH}_4/\text{SiD}_4$	2186.87/1563.3(cm^{-1})[10]	1.399
$^{12}\text{C}/^{13}\text{C}$	1332,5/1280(cm^{-1})[10;25]	1.041
$^{70}\text{Ge}/^{76}\text{Ge}$	309.8/297.7(cm^{-1})[10,26,27]	1.041
$^{28}\text{Si}/^{30}\text{Si}$	524.8/509.8(cm^{-1})[28]	1.029
$^{64}\text{Zn}/^{76}\text{Se}/^{68}\text{Zn}/^{80}\text{Se}$	213.2/207.4(cm^{-1})[10]	1.028
$\alpha-^{112}\text{Sn}/\alpha-^{124}\text{Sn}$	206.5/196.8(cm^{-1})[10,30]	1.049
$\text{Ga}^{14}\text{N}/\text{Ga}^{15}\text{N}$	535/518(cm^{-1})[10,31]	1.033
$^{63}\text{Cu}/^{35}\text{Cl}/^{65}\text{Cu}/^{37}\text{Cl}$	174.4/171.6(cm^{-1})[10,32]	1.016